



City Research Online

## City, University of London Institutional Repository

---

**Citation:** Nomoni, M., May, J.M. & Kyriacou, P. A. (2020). Fabricating Novel PDMS Vessels for Phantoms in Photoplethysmography Investigations. 2020 42nd Annual International Conference of the IEEE Engineering in Medicine & Biology Society (EMBC), 2020(July), pp. 4458-4461. doi: 10.1109/EMBC44109.2020.9176476 ISSN 1557-170X doi: 10.1109/EMBC44109.2020.9176476

This is the accepted version of the paper.

This version of the publication may differ from the final published version.

---

**Permanent repository link:** <https://openaccess.city.ac.uk/id/eprint/25045/>

**Link to published version:** <https://doi.org/10.1109/EMBC44109.2020.9176476>

**Copyright:** City Research Online aims to make research outputs of City, University of London available to a wider audience. Copyright and Moral Rights remain with the author(s) and/or copyright holders. URLs from City Research Online may be freely distributed and linked to.

**Reuse:** Copies of full items can be used for personal research or study, educational, or not-for-profit purposes without prior permission or charge. Provided that the authors, title and full bibliographic details are credited, a hyperlink and/or URL is given for the original metadata page and the content is not changed in any way.

---

City Research Online:

<http://openaccess.city.ac.uk/>

[publications@city.ac.uk](mailto:publications@city.ac.uk)

---

# Fabricating Novel PDMS Vessels for Phantoms in Photoplethysmography Investigations

Michelle Nomoni, James M. May, Member IEEE and Panayiotis A. Kyriacou, Senior Member IEEE

**Abstract**— This paper introduces a novel technique for the development of custom polydimethylsiloxane (PDMS) vessels for use in phantom technologies. The method involves continuous dip coating of commercial silicone tubes with rapid curing in a single controlled process. The technique accommodates the production of different vessel diameters, wall thicknesses (56  $\mu\text{m}$ –80  $\mu\text{m}$ ) and mechanical properties. Clear phantoms were fabricated to compare the commercial silicone tubes against the custom vessels. A pulsatile fluidic pump (BDCLabs, CO, USA) driven by a computer controlled linear motor generated the pulsatile flow through the phantom. The resulting flow profile, using the custom vessels, simulates human blood flow and the detected contact PPG signal from the phantom closely resembles the morphology of *in vivo* PPG waveforms with signal-to-noise ratios of 38.16 dB and 40.59 dB, compared to the closest commercially-available tubing at 5.38 dB and 10.59 dB for the red and infrared wavelengths respectively. The rigidity and thick walls of commercial silicone tubes impede the expansion of the tubing under systolic pressure. This technique eliminates this common limitation in phantom development.

## I. INTRODUCTION

The optical technique photoplethysmography (PPG) is used to measure several haemodynamics properties with well-established applications in clinical monitoring [1]. The resurgent interest of PPG devices in the last decade stems from the growing demand for wearable health sensors, for example smart watches or exercise bands that provide non-invasive assessment of cardiovascular physiology [2]. The adoption of phantom technologies for the testing and evaluation of biophotonic sensors will help deploy new technologies for clinical and commercial use more rapidly through increased reliability and results reproducibility. Phantoms also allow in-depth research into isolated parameters of physiology that contribute to the origin of the PPG signal [3], [4].

The most common PPG technology, pulse oximetry relies solely on *in vivo* blood samples for calibration, a process which is costly and time consuming [5]. Phantoms are already implemented in medical imaging for calibration of CAT-scans, ultrasound and MRI machines, they provide high repeatability, and through design of layered structures, different physiology can be represented [6]. These desirable qualities should be utilised to create a standard phantom against which optical sensors such as PPGs can be evaluated and calibrated with.

M. Nomoni, J. M. May and P. A. Kyriacou are with the School of Mathematics, Computer Science and Engineering, City, University, of London, EC1V 0HB, UK (e-mail: michelle.nomoni.1@city.ac.uk).

The literature on tissue mimicking phantom materials is extensive, and over the years several custom multi-modal phantoms have been described [7], [8]. Liu et al describes the effects of India ink, Intralipid, glycerol, gelatine and other substances as absorption and scattering attenuators [9]. These phantoms serve many functions, to initially test systems, to optimise signal-to-noise ratios (SNR) in their development stage and to compare existing systems against one another. Regulatory bodies such as the American College of radiology (ACR) often approve new systems based on their performance against quality control phantoms, this is an established criterion in medical imaging devices. Commercial manufacturers with their considerable resources and production experience are able to produce high quality phantoms for industrial purposes, but during the developmental stage of new systems at research institutes, the phantoms being produced have been found to be inconsistent, their properties change over time, and have low reproducibility [10].

A common limitation of phantoms which incorporate pulsatile flow with artificial vessels is the mechanical response of commercially available silicone tubing. When blood vessels expand under systolic pressure, the increased volume of blood is the leading origin of the PPG signal. Thick walls and stiff silicone inhibit this expansion and as a result, reduce the volume variation leading to the detection of weak PPG signals. This limitation was faced in continuation of previous phantom work, larger brachial sized tubing produces satisfactory PPG results, but when the size of tubing was reduced to only the palmar arch size, the PPG's became very weak and almost undetectable [11]. This led to the development of the novel technique described in this paper to produce thin walled vessels that produce high quality PPG signals.

## II. METHODS

This section establishes the novel technique used to fabricate custom PDMS vessels with comparable wall thicknesses to real blood vessels. The placement of these vessels into a medium of artificial tissue is described, and the pump system design that allows parameter control is outlined.

### A. Fabrication of Custom Vessels

Each human finger is supplied with blood from two digital arteries, the radial and ulnar digital arteries. Leslie et al measures the average diameter of the largest digital artery to be 1.44 mm [12]. The intima-media thickness (IMT) of digital arteries could not be found, but the nearest vessel, the superficial palmar arch artery is measured to have an IMT of 105  $\mu\text{m}$  [13]. No commercial tubing are available at these

values, or they are prohibitively expensive to have custom-made. Many other research groups have also faced challenges using commercially available tubing as vessel substitutes and have endeavoured to fabricate their own custom vessels from varying materials and methods [14]. Therefore, a unique fabrication method has been developed by the research team.

To produce a thin walled vessel, a continuous dip coating technique has been developed; A precision dip coater (Qualtech, UK) was adapted to fabricate the vessels. Silicone tubing of 1.3mm internal diameter (ID) (Hilltop-Products, UK) was attached to the arm of the dip coater and threaded through the heating coil. It is then passed through the trough below. The tubing is then hung across a series of pulleys with a tension weight attached at its end. The trough is then filled with PDMS (Sylgard 184, Dowsil, UK) chosen for its long pot life of 2 hours and fast cure rate. Figure 1 is a diagrammatic representation of this setup.

A long pot life ensures high yield per batch before replacement of PDMS is required, and the fast cure-rate results in a shorter time required passing through the heating coil allowing faster withdrawal rates. Once the system arrangement was complete, the heating-coil was switched on to increase the air temperature to 275 C. The dip coater system then progressed the tubing at a steady rate of 10 mm.min<sup>-1</sup>, to evenly coat the tubing. The coated section of tubing then passed through the heating element, where the coating cured. After the dip coater reached maximum withdrawal length, the tubing was cut, and the arm was reset back to its minimum position. The cut length of coated tubing was placed in an infrared reflow oven set at 150 C for 10 minutes to ensure a complete and thorough cure. The coating was then separated from the internal tubing. This method produced custom vessels with inner diameters that are equivalent to the outer diameter of the internal tubing, and wall thicknesses that can be adjusted by varying the speed of withdrawal. The mechanical properties could also be varied by altering the catalyst ratio of the PDMS that results in different shore hardnesses.

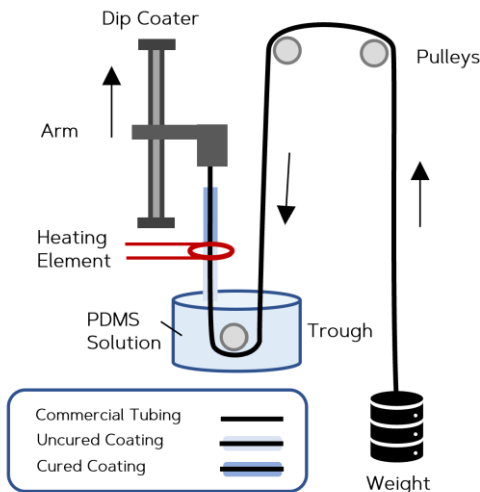


Figure 1 Continuous dip coating fabrication method.

## B. Phantom Assembly

The phantom was modelled after the finger, where typically PPG sensors are placed for pulse oximetry. The digital arteries sit within fat and tendons with varied optical and mechanical properties. To simplify the phantom design at this stage, where vessels are being investigated, the chosen model consisted of either a custom or commercial vessel surrounded by homogenous clear PDMS. A rectangular container with the approximate dimensions of a finger was 3D printed (Formlabs, MA, U.S.). The 70 mm x 15 mm x 15 mm open-top container consisted of holes on either end to have the vessel passed through. The vessel was threaded through the container and at one side and secured in place using UV hardened high temperature glue. The other end of the vessel was stretched taut and secured. The glue acted as a plug to avoid drainage during the curing process. The silicone tissue mixture was then poured into the container and cured at 150°C for 10 minutes. The phantom was then cooled before connecting the vessels to connectors and the fluid distribution network.

## C. In vitro System

The set up for the *in vitro* experiment follows the Windkessel model, a widely used model for estimating the overall compliance of a systematic arterial system [15]. Figure 2 shows the diagrammatic representation of all major components. The pump is a pulsatile fluidic pump from BDC Labs (CO, U.S.A.), driven by a computer-controlled linear motor. The resistance elements mimic the Iliac resistance component and the total peripheral resistance (TPR) which causes vessels to store energy during systole and release a secondary pressure wave, a distinct dichroitic notch detected in PPG. The pulsatile fluid used in these set of experiments was a phosphate buffer solution with India ink (Bombay Black, Dr. Ph. Martins, UK) as a base absorber.

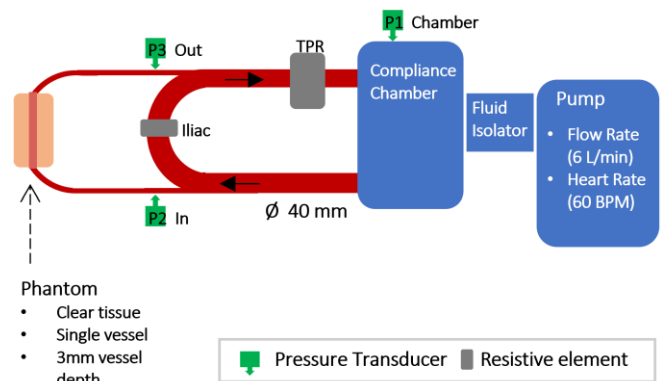
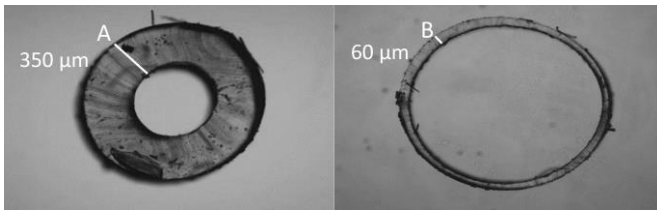


Figure 2 In vitro pump system

## III. RESULTS

The design of custom vessels was a new technique established as a solution to limitations faced in the development of phantoms. The key variable explored at this stage was the rate of withdrawal. To investigate the effects of the rate of withdrawal, four speeds were chosen 5, 10, 15,

and 20 mm.min<sup>-1</sup>. To measure the variability, 1000 mm of custom vessels were produced at each speed, 25 slices were taken along its length and placed under a microscope to take wall thickness measurements using YenCAM (YenWay, UK), see figure 3.



**Figure 3** Microscopic images of vessel cross sections. (A) Commercial vessel (ID = 0.7 mm). (B) Custom Vessel (ID = 1.4 mm) withdrawn at 10 mm.min<sup>-1</sup>.

Analysis was performed using MATLAB® (The MathWorks, USA) to determine the effect of withdrawal speed on wall thickness and variability. The boxplot in figure 4 displays the distribution of wall thickness at the withdrawal speeds of 5 to 20 mm.min<sup>-1</sup>. The median wall thickness shows a positive correlation with withdrawal speed and demonstrates the effect that withdrawal speed has on the variability of wall thickness measurements. Both commercial (OD = 1.4 mm) and custom vessels (OD = 1.52 mm) were embedded into separate phantom moulds and encased within clear silicone tissue.

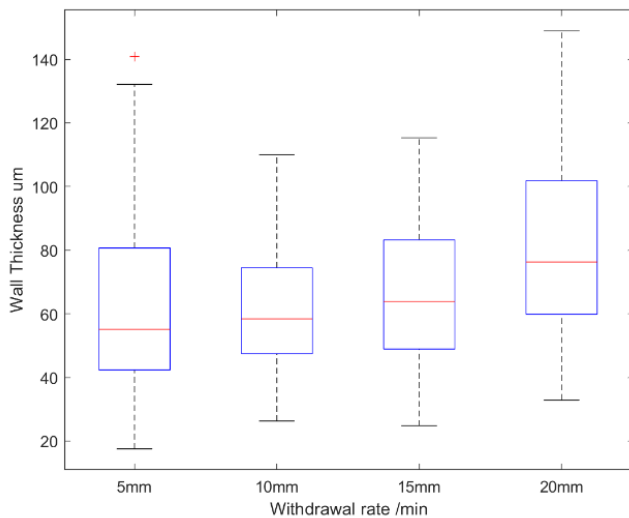


**Figure 4** Box plot of the wall thickness at different withdrawal rates.

Clear tissue was chosen at this stage to eliminate further variables affecting the resultant signals. The phantoms were connected to the *in-vitro* system and a pulsatile flow was introduced into the phantoms. PPG data was collected from the sensor (OSRAM SFH 7050) placed above the surface of the phantom. The PPG of both phantoms were recorded in Labview (National Instruments, U.S.) and are compared in figure 5.

For the first time a vessel-tissue phantom has been produced with geometrically vessels. When integrated into a

pulsatile pump the tissue exhibited similar morphological features to a physiological PPG signal with similar signal to noise ratios [16].

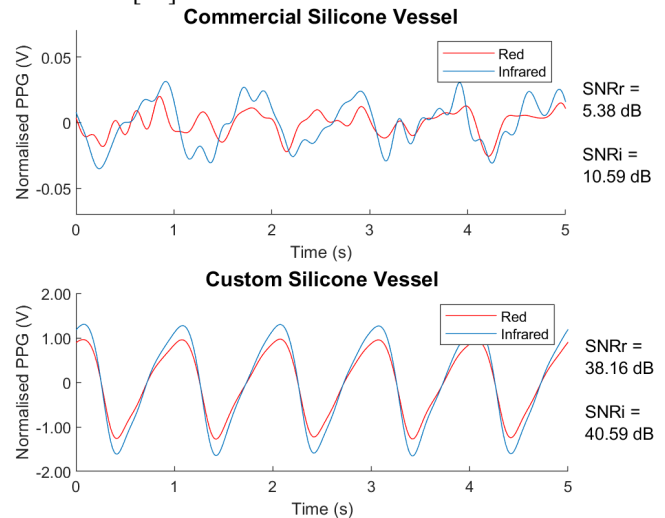


**Figure 5** The PPG signal from the clear vessel phantoms. Top: Commercial vessels. Bottom: Custom vessels

The custom vessels were produced at four withdrawal speeds, which had an impact on two factors. First, the time between leaving the solution and entering the heating element. This had a role on the final thickness of the coating which in turn would be the wall thickness of the final vessel. Second, the time spent curing in the heating element. If the vessel did not spend enough time in heating element, it would not fully cure, and variability increased as a result. Experimentally the 5 mm.min<sup>-1</sup> speed produced vessels with the highest variability, and 20 mm.min<sup>-1</sup> produced the thickest walls. The results show that a speed of 10 mm.min<sup>-1</sup> was best to provide an even cure across the length of vessels and that faster speeds had little impact on wall thickness but did increase the variability of wall thickness on a single vessel.

Chen et al discuss in their phantom development process that commercial vessels were a major hindrance in phantom quality and that future work would involve self-fabrication of vessels [14]. The cross section in figure 3, of the commercial and custom vessel, shows that thin walls are achievable, and the results in reproducibility, in small batches, is enough to satisfy the production of a small number of custom phantoms for investigative purposes. The commercial silicone vessels are measured to have a 350 μm walls and the custom vessels withdrawn at a speed of 10 mm.min<sup>-1</sup> have a median wall thickness of 60 μm.

This reduction in wall thickness, increases the elasticity and therefore compliance of the vessel. The PPG signals obtained from the commercial vessel phantoms had low SNR's, 5.38 dB and 10.59 dB in red and infrared wavelengths respectively, with no morphology of the PPG waveform observed. In comparison the custom vessel phantom produces high SNR's of 38.16 dB and 40.59 dB for the red and infrared wavelengths respectively.

#### IV. CONCLUSION

For the first time a vessel-tissue phantom has been produced with geometrically and mechanically accurate vessels. When integrated into a pulsatile pump the tissue exhibited similar morphological features to a physiological PPG signal with similar signal to noise ratios [17], [18]. The development of these vessels, and its validation through fundamental investigations are a step towards developing advanced phantoms to aid in standardising the evaluation of PPG systems and sensors. There is no current criterion or industry standard phantom for which PPG technology is assessed against.

#### REFERENCES

- [1] J. Allen, "Photoplethysmography and its application in clinical physiological measurement," *Physiol. Meas.*, vol. 28, no. 3, pp. R1–R39, 2007.
- [2] T. Tamura, Y. Maeda, M. Sekine, and M. Yoshida, "Wearable Photoplethysmographic Sensors—Past and Present," *Electronics*, vol. 3, no. 2, pp. 282–302, 2014.
- [3] C. I. Nwafor *et al.*, "Assessment of a noninvasive optical photoplethysmography imaging device with dynamic tissue phantom models," *J. Biomed. Opt.*, 2017.
- [4] V. V. Tuchin, "Tissue Optics and Photonics: Biological Tissue Structures," *J. Biomed. Photonics Eng.*, 2015.
- [5] T. Aoyagi, "Pulse oximetry: its invention, theory, and future," *J. Anesth.*, vol. 17, no. 4, pp. 259–266, Nov. 2003.
- [6] M. O. Culjat, D. Goldenberg, P. Tewari, and R. S. Singh, "A review of tissue substitutes for ultrasound imaging," *Ultrasound in Medicine and Biology*, vol. 36, no. 6, pp. 861–873, 2010.
- [7] S. Kleiser, N. Nasser, B. Andresen, G. Greisen, and M. Wolf, "Comparison of tissue oximeters on a liquid phantom with adjustable optical properties," *Biomed. Opt. Express*, vol. 7, no. 8, p. 2973, Aug. 2016.
- [8] M. Paul, A. F. Mota, C. H. Antink, V. Blazek, and S. Leonhardt, "Modeling photoplethysmographic signals in camera-based perfusion measurements: optoelectronic skin phantom," *Biomed. Opt. Express*, vol. 10, no. 9, p. 4353, Sep. 2019.
- [9] G. Liu *et al.*, "Fabrication of a multilayer tissue-mimicking phantom with tunable optical properties to simulate vascular oxygenation and perfusion for optical imaging technology," *Appl. Opt.*, vol. 57, no. 23, p. 6772, Aug. 2018.
- [10] B. W. Pogue and M. S. Patterson, "Review of tissue simulating phantoms for optical spectroscopy, imaging and dosimetry," *J. Biomed. Opt.*, vol. 11, no. 4, p. 041102, 2006.
- [11] M. Nomoni, J. M. May, and P. A. Kyriacou, "A Pulsatile Optical Tissue Phantom for the Investigation of Light-Tissue Interaction in Reflectance Photoplethysmography," in *2019 41st Annual International Conference of the IEEE Engineering in Medicine and Biology Society (EMBC)*, 2019, vol. 2019, pp. 3204–3207.
- [12] B. M. Leslie, L. K. Ruby, S. J. Madell, and F. Wittenstein, "Digital artery diameters: an anatomic and clinical study," *J. Hand Surg. Am.*, vol. 12, no. 5 Pt 1, pp. 740–3, Sep. 1987.
- [13] A. N. Pruzan, A. E. Kaufman, C. Calcagno, Y. Zhou, Z. A. Fayad, and V. Mani, "Feasibility of imaging superficial palmar arch using micro-ultrasound, 7T and 3T magnetic resonance imaging," *World J. Radiol.*, vol. 9, no. 2, pp. 79–84, Feb. 2017.
- [14] A. I. Chen *et al.*, "Multilayered tissue mimicking skin and vessel phantoms with tunable mechanical, optical, and acoustic properties," *Med. Phys.*, vol. 43, no. 6, pp. 3117–3131, 2016.
- [15] N. Westerhof, G. Elzinga, and P. Sipkema, "An artificial arterial system for pumping hearts," *J. Appl. Physiol.*, vol. 31, no. 5, pp. 776–81, Nov. 1971.
- [16] J. M. May, J. P. Phillips, T. Fitchat, S. Ramaswamy, S. Snidvongs, and P. A. Kyriacou, "A Novel Photoplethysmography Sensor for Vital Signs Monitoring from the Human Trachea," *Biosensors*, vol. 9, no. 4, Oct. 2019.
- [17] A. P. Yoganathan *et al.*, "Comparison of NIRS, laser Doppler flowmetry, photoplethysmography, and pulse oximetry during

vascular occlusion challenges," *Physiol. Meas.*, vol. 36, no. 5, pp. 503–514, 2016.

- [18] M. Elgendi, "On the Analysis of Fingertip Photoplethysmogram Signals," *Curr. Cardiol. Rev.*, 2012.